Philosophical Magazine
Publication details, including instructions for authors and subscription information:
http://www.tandfonline.com/loi/tphm20

Atomistic scale fracture behaviours in hierarchically nanotwinned metals

Fuping Yuan [a] & Xiaolei Wu [a]
[a] State Key Laboratory of Nonlinear Mechanics, Institute of Mechanics, Chinese Academy of Science , Beijing , 100190 , People's Republic of China
Published online: 30 May 2013.

To cite this article: Fuping Yuan & Xiaolei Wu (2013) Atomistic scale fracture behaviours in hierarchically nanotwinned metals, Philosophical Magazine, 93:24, 3248-3259, DOI: 10.1080/14786435.2013.805278

To link to this article: http://dx.doi.org/10.1080/14786435.2013.805278

Philosophical Magazine, 2013
Vol. 93, No. 24, 3248–3259, http://dx.doi.org/10.1080/14786435.2013.805278

Atomistic scale fracture behaviours in hierarchically nanotwinned metals

Fuping Yuan* and Xiaolei Wu

State Key Laboratory of Nonlinear Mechanics, Institute of Mechanics, Chinese Academy of Science, Beijing 100190, People's Republic of China

(*Received 19 March 2013; final version received 3 May 2013*)

In the present study, a series of large-scale molecular dynamics simulations have been performed to investigate the atomistic scale fracture behaviours along the boundaries of primary twins in Cu with hierarchically nanotwinned structures (HTS), and compare their fracture behaviours with those in monolithic twins. The results indicate that crack propagation along [1 1 2] on the twin plane in monolithic nanotwins is brittle cleavage and fracture, resulting in low crack resistance and fracture toughness. However, the crack resistance along the boundaries of primary twins in HTS is much higher, and a smaller spacing of secondary twins (λ_2) leads to even higher fracture toughness. With large λ_2, the crack growth is achieved by void nucleation, growth and coalescence. However, considerable plastic deformation and enhanced fracture toughness in HTS could be achieved by the crack blunting and by the extensive dislocation accommodation ahead of the crack tip when λ_2 is small.

Keywords: molecular dynamics simulations; fracture; crack growth; twins; hierarchically nanotwinned structures

1. Introduction

The emergence of an observable fracture is a consequence of crack propagation across several widely different length scales, i.e. from atomistic to continuum scales. A number of milestone theories and models of fracture mechanics have been developed and a framework of continuum fracture mechanics has been well established at the macroscopic scale over the last century [1–5]. Although molecular dynamics (MD) simulations have been used for many years now to study crack-tip response in various materials [6–21], fracture behaviour at the nanometre scale is still much less understood. Fracture behaviour at the atomistic scale is strongly dependent on the atomistic structure, such as grain size, grain boundary (GB), twin boundary (TB) and lattice orientation [6–23].

Efforts have been undertaken to improve the strength and toughness of materials by tailoring microstructures [24–27], via severe plastic deformation techniques. Experimentally, the hierarchically twinned structures (HTS) could be achieved in these materials, as evidenced in the samples processed with the newly developed techniques with high

*Corresponding author. Email: fpyuan@lnm.imech.ac.cn

strain rates and/or low temperatures, such as dynamic plastic deformation [28–29], surface mechanical attrition treatment (SMAT) [30–31] and surface mechanical grinding treatment (SMGT) [32]. For example, the secondary twins could be generated in the primary twins in the twinning-induced plasticity (TWIP) steels [33] and 304 stainless steels [34] during the process of SMAT. Experiments have also shown that high rate and low temperature deformation (such as SMGT) may lead to the formation of secondary twins inside primary twin/matrix lamellae in those fcc metals with medium stacking faults (SF) energy such as Cu [34]. The boundaries for primary twins in the deformation-induced HTS are split by secondary twins and no longer coherent. Recent experiments have shown that the hierarchically twinned structures with the secondary twins at the nanoscale can be a novel nanostructured design to achieve higher strength and toughness. So, the objective of the present study is to reveal the atomistic scale fracture behaviours along the boundaries for primary twins in Cu with HTS, and compare their fracture behaviours with those in monolithic twins, using a series of large-scale MD simulations.

2. Simulation procedure

The MD simulations were carried out using the Large-Scale Atomic/Molecular Massively Parallel Simulator code and a Cu EAM potential developed by Mishin et al. [35]. This potential was calibrated according to the *ab initio* values of stacking fault and twin formation energies. Constrained three-dimensional atomistic model with a single-edge crack is employed to investigate the phenomena of nanoscale fracture under a mode I loading condition. The thickness direction contains 12 atomic planes, and is along $[\bar{1}\ 1\ 0]$. Four samples with the same size of $100 \times 83.5 \times 1.66\,\text{nm}^3$ ($\sim$1080,000 atoms) were considered for comparison, and an ellipse-shaped initial crack with a length of 10 nm (10% of the sample length) was introduced in each sample. Sample I represents crack propagation along the TB in the monolithic nanotwinned crystal, with a TB spacing of 10.44 nm. Samples II, III and IV represent crack propagation along the boundaries of primary twins in HTS. The TB spacing of primary twins (λ_1) is 10.44 nm for samples II, III and IV. However, the TB spacing of secondary twins (λ_2) is 10.44, 4.17 and 2.09 nm in samples II, III and IV, respectively. Before loading, the as-created samples were first subject to energy minimization by the conjugate gradient method; then gradually heated up to the desired temperature in a stepwise fashion; and finally relaxed in the Nose/Hoover isobaric-isothermal ensemble under both the pressure 0 bar and the desired temperature (1 K) for 100 ps. To visualize defects, atoms were coloured according to common neighbour analysis values [36]. Grey colour stands for perfect fcc atoms; red colour stands for hcp atoms; and green colour stands for GBs, dislocation core, free surface and other atoms. A single line of hcp atoms represents a TB; two adjacent hcp lines stand for an intrinsic stacking fault, and two hcp lines with an fcc line between them indicates an extrinsic stacking fault. The relaxed sample with monolithic nanotwins is shown in Figure 1(a), while the typical relaxed sample with HTS ($\lambda_1 = 20.87$ nm, $\lambda_2 = 4.17$ nm) is shown in Figure 1(b). As shown in Figure 1(c), the twin boundaries for the primary twins are split into TB_{1st} and GB_{1st} when the secondary twins are generated in the primary twins. As shown in Figure 1(d), both TB_{1st} and GB_{1st} are symmetrical $[\bar{1}\ 1\ 0]$ tilt GBs, in which TB_{1st} is special TB with $\sum 3(1\ 1\ 1)$

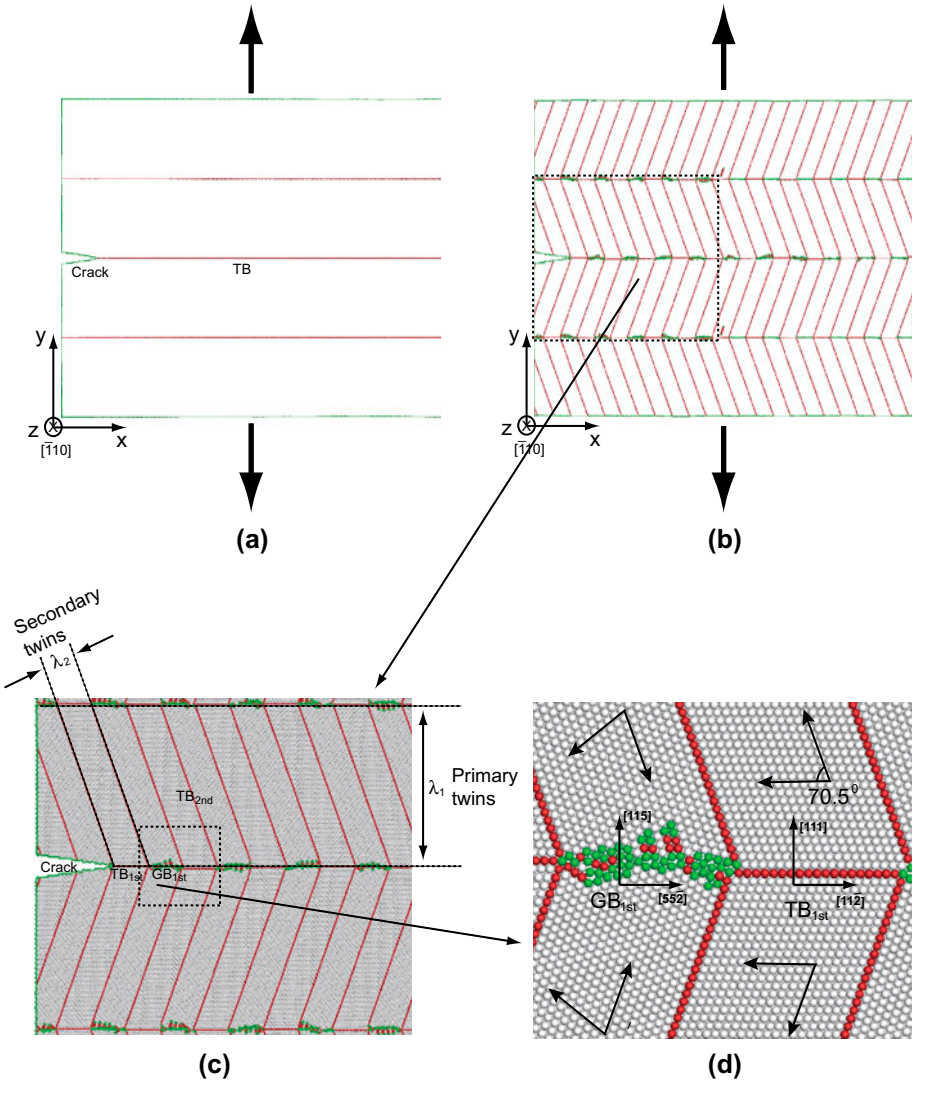

Figure 1. (colour online) (a) The relaxed sample with monolithic nanotwins: $\lambda_1 = 20.87$ nm (perfect fcc atoms are not shown in this figure). (b) The relaxed sample with hierarchically twinned structures: $\lambda_1 = 20.87$ nm, $\lambda_2 = 4.17$ nm (perfect fcc atoms are not shown in this figure). (c) The corresponding amplified configuration for Figure 1(b) showing the details for the initial crack, primary twins and secondary twins. (d) The corresponding amplified configuration for Figure 1(c) show the details for TB_{1st} and GB_{1st}, and the slip planes are also marked in the Figure.

and GB_{1st} is a boundary with $\sum 27(1\ 1\ 5)$. For all as-created samples with HTS, the TB_{1st} is always right in front of crack-tip. The relaxed samples were then loaded by an opening incremental displacement of 0.021 nm every 1 ps (which results in a global strain of 0.05%) along the top and bottom edges. After each loading step, the top and bottom boundary atoms are fixed while the remaining atoms are allowed find their

equilibrium positions for 15 ps. During the loading process, a periodic boundary condition was imposed in the out-of-plane direction (Z direction), while the displacement in the X direction along the right boundary was constrained to zero in order to limit boundary effects.

3. Results and discussions

Figure 2(a) shows the engineering stress–strain curves obtained for all four pre-cracked samples. Figure 2(b) shows the results for the effective crack-tip extension as a function of strain for all four pre-cracked samples. The effective crack-tip extension is calculated by the newly created surface length along the boundaries of primary twins. Samples I, II and III are strained until the overall crack length reaches the half length of the sample length. However, a strain of 10% is applied to the sample IV, since the sample IV is

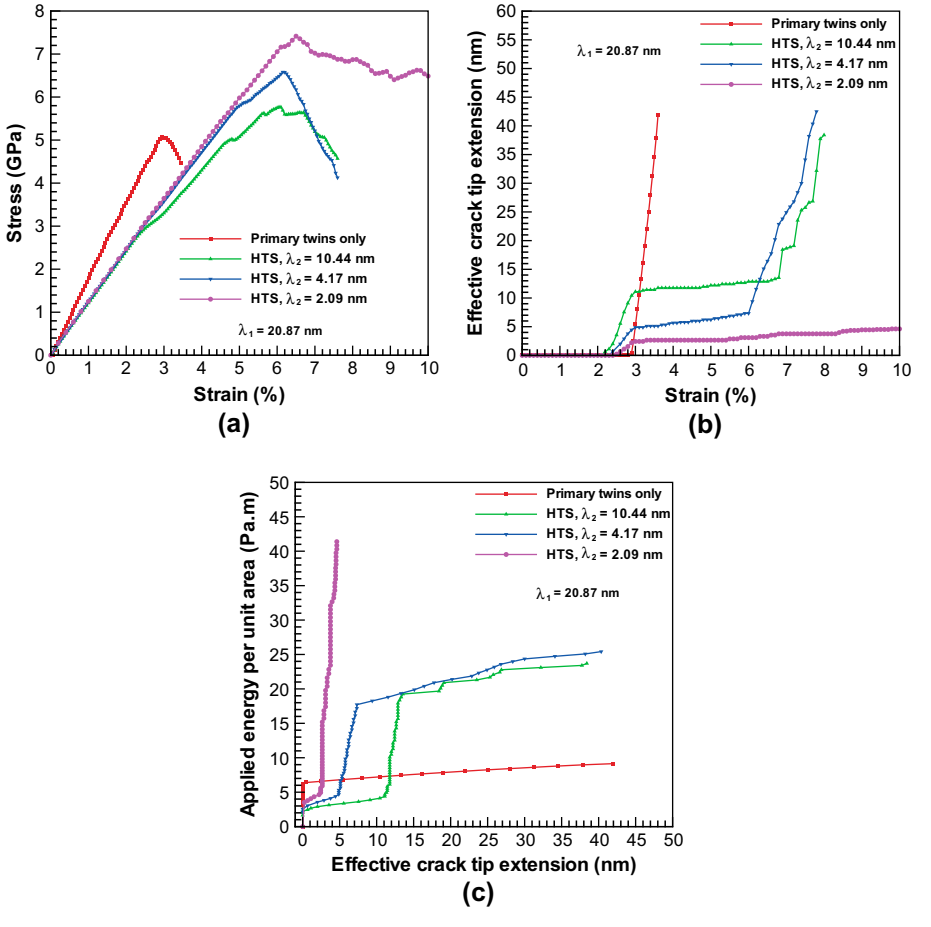

Figure 2. (colour online) (a) Simulated stress-strain curves for all pre-cracked samples. (b) Effective crack-tip extension as a function of strain for all pre-cracked samples. (c) Applied strain energy per unit area as a function of effective crack-tip extension for all pre-cracked samples.

much tougher and the overall crack length is less than 20% even when the strain is as high as 10%. In order to quantitatively show the effect of spacing of secondary twins on the crack resistance, the applied strain energy per unit area as a function of effective crack-tip extension for all pre-cracked samples is plotted in Figure 2(c). The results clearly indicate that a smaller spacing of secondary twins leads to higher crack resistance and fracture toughness for HTS, which is also much higher than those of monolithic nanotwins. Detail atomistic microstructure and stress field around and ahead of the crack tip will be presented below in order to illustrate the toughening mechanisms of HTS.

As shown in Figure 2(a), the peak stresses of the samples with HTS are higher than those of the sample with monolithic nanotwins, and increase when λ_2 decreases. In order to reveal the underlying deformation mechanisms, the deformed configurations at the peak stress for the sample with monolithic nanotwins and for the samples with HTS ($\lambda_1 = 20.87$ nm, $\lambda_2 = 4.17$ nm; $\lambda_1 = 20.87$ nm, $\lambda_2 = 2.09$ nm) are shown in Figure 3. For all samples, the strain at the peak stress corresponds to the onset of crack propagation. It is clearly seen that no dislocation behaviours are observed for the sample with monolithic nanotwins at onset of crack propagation, resulting in brittle cleavage and lower peak strength. For the samples with HTS, the initial crack propagation is along the first TB_{1st}, and then the early stage of crack-tip blunting is observed at the first GB_{1st} at the strain for peak stress. Apparently, the smaller λ_2 should give larger resistance for the dislocation slips around the crack tip at onset of crack-tip blunting, which resulting in larger peak stress.

Figure 4(a)–(d) shows a sequence of simulated snapshots illustrating crack propagation along the TB in the monolithic nanotwins. It is observed that crack is propagated without emitting dislocations from crack tip, indicating brittle cleavage and fracture. It is well known that a void is nucleated where the mean stress has peak value [17]. It is also well know that the dislocation behaviours along the boundaries are controlled by the resolved shear stress on the boundaries. Stress contours ($\sigma_{yy}, \sigma_{mean}, \sigma_{xy}$) near the crack-tip region of the monolithic nanotwins at two different strains are shown in

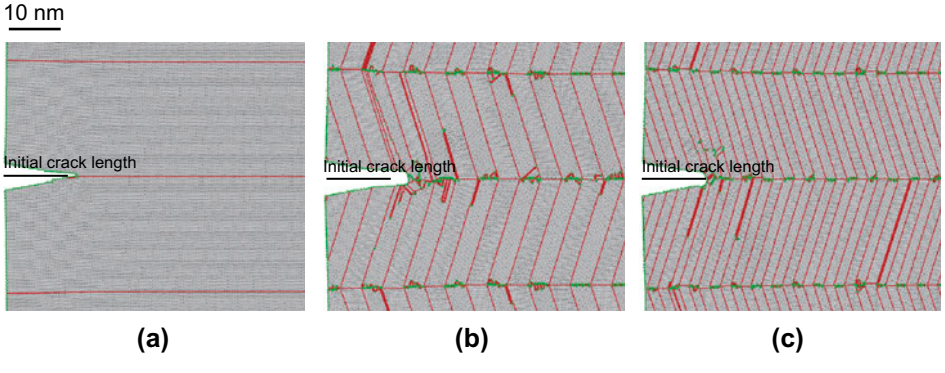

Figure 3. (colour online) The deformed configurations at the peak stress for: (a) the sample with monolithic nanotwins; (b) the sample with hierarchically twinned structures of $\lambda_1 = 20.87$ nm, $\lambda_2 = 4.17$ nm; (c) the sample with hierarchically twinned structures of $\lambda_1 = 20.87$ nm, $\lambda_2 = 2.09$ nm. The initial crack length is also marked in the Figure.

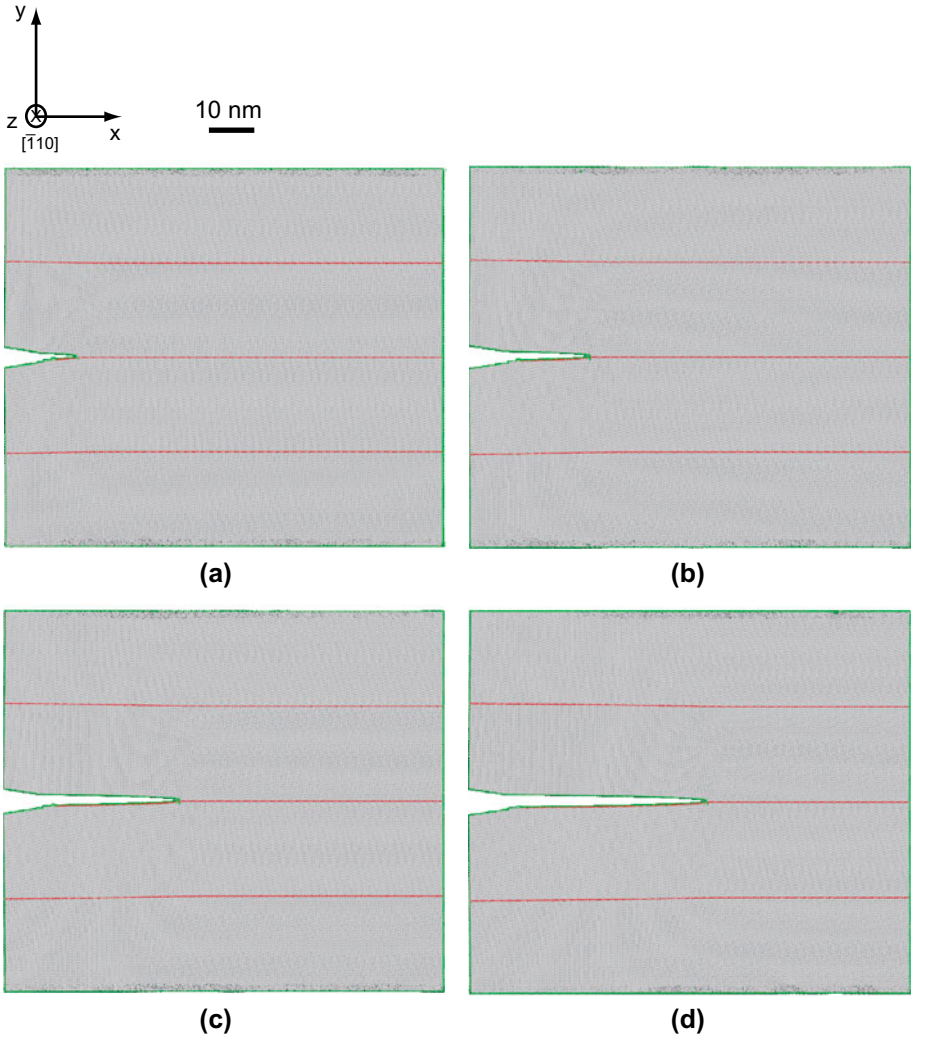

Figure 4. (colour online) Simulated snapshots illustrating crack propagation along the TB in the monolithic nanotwins: (a) at a strain of 3.0%; (b) at a strain of 3.2%; (c) at a strain of 3.4%; (d) at a strain of 3.6%.

Figure 5(a)–(b). Both the mean stress σ_{mean} and the tensile stress σ_{yy} have peak values right ahead of crack tip, and as high as 10 and 5 GPa respectively. This large tensile stress results in creating new surfaces and crack propagation. The maximum resolved shear stress on the TB is about 0.7 GPa, which is much smaller than the critical shear stress (2.16 GPa) required to nucleate partial dislocations from the TB. An interesting directional anisotropy of the fracture mode along a coherent TB $\sum 3[1\ \bar{1}\ 1]$ in Cu, i.e. brittle cleavage for a crack moving along $[1\ \bar{1}\ \bar{2}]$ in the twin plane but dislocation emission for moving in the perpendicular direction, has also been observed from recent theoretical and atomistic study [18,21]. The energy release rate associated with brittle cleavage along a TB can be written as

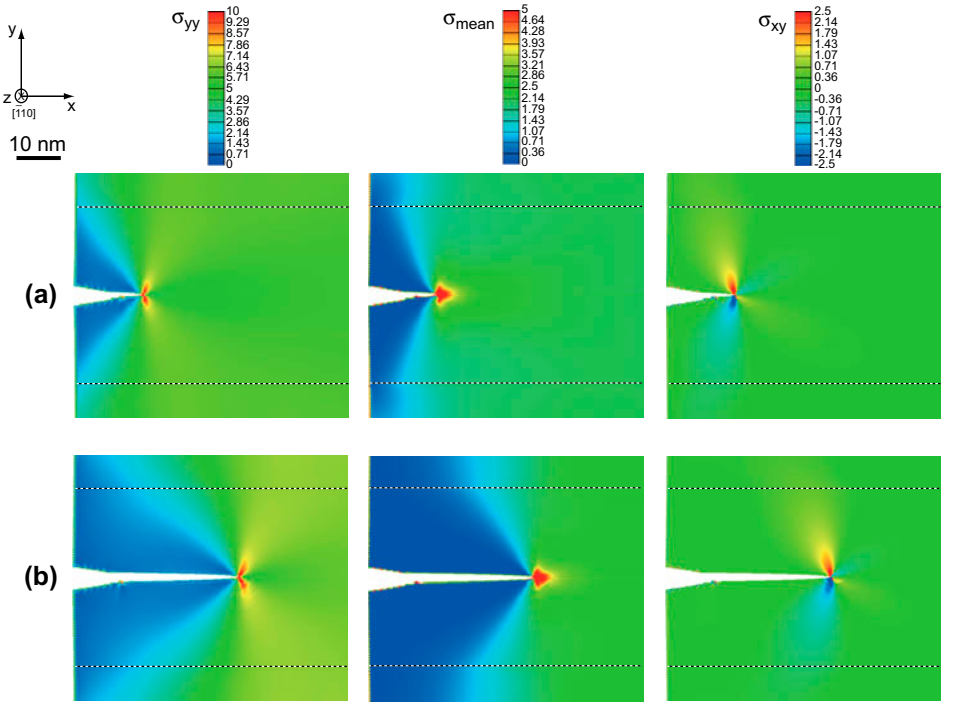

Figure 5. (colour online) Stress contours ($\sigma_{yy}, \sigma_{mean}, \sigma_{xy}$) near the crack-tip region of the monolithic nanotwins: (a) at a strain of 3.0%; (b) at a strain of 3.4%. The black dash lines in the figure are twin boundaries.

$$G = 2\gamma_s - \gamma_{tb} \tag{1}$$

where γ_s and γ_{tb} are the fracture surface energy and the TB energy, respectively. So, the critical stress intensity factor at the crack tip is

$$K_{Ic} = \sqrt{\frac{2G\mu}{1-\nu}} = \sqrt{\frac{2\mu(2\gamma_s - \gamma_{tb})}{1-\nu}} \tag{2}$$

where μ and ν are the shear modulus and the Poisson ratio, respectively. The mode-I asymptotic crack-tip shear stress field has the following expression,

$$\tau_{xy} = \frac{K_{Ic}}{\sqrt{2\pi r}} \cos\frac{\theta}{2} \sin\frac{\theta}{2} \cos\frac{3\theta}{2} \tag{3}$$

where r and θ are polar coordinates surrounding the crack tip. Although Equation (3) is for isotropic materials, a rough estimate for the resolved shear stress on the TB can still be made for our case. It can be concluded that the resolved shear stress has its maximum at $\theta \approx 108^\circ$ on the TB, i.e.

$$|\tau_{tb}|_{\max} = 0.441\sqrt{\frac{\mu(2\gamma_s - \gamma_{tb})}{\pi\lambda_1(1-\nu)}} \tag{4}$$

Substituting the material parameters from literatures [21] into Equation (4), the resolved shear stress on the TB should be smaller than 1 GPa when $\lambda_1 = 10.44$ nm, which is consistent with our simulation results. This suggests that coherent twin boundaries are intrinsically brittle and could serve as cleavage planes when the TB spacing is large.

Figure 6(a)–(d) shows a sequence of simulated snapshots illustrating crack propagation along the boundaries of primary twins in HTS ($\lambda_1 = 20.87$ nm, $\lambda_2 = 4.17$ nm). Since the deformation mechanisms and fracture behaviours for samples with $\lambda_2 = 4.17$ nm and $\lambda_2 = 10.44$ nm are very similar, only the simulated snapshots for the sample with $\lambda_2 = 4.17$ nm are shown here. In contrast to monolithic nanotwins, hierarchically nanotwinned metals possess two characteristic microstructural length scales (the spacing for primary twins λ_1 and the spacing for secondary twins λ_2) and various boundaries, such as GB_{1st}, TB_{1st} and TB_{2nd} (Figure 6(a)). From the simulation results, it is observed that crack growth in HTS is achieved by four stages when λ_2 is large: (i) initial crack growth along first TB_{1st} (Figure 6(a)); (ii) crack-tip blunting at GB_{1st} (Figure 6(b) and (c)); (iii) void nucleation and growth from other sites of TB_{1st} (Figure 6(d) and (e)); and (iv) void coalescence and crack growth (Figure 6 (f)). From Figure 6(a)–(d), it is observed that partial dislocations are emitted from GB_{1st} and no dislocations are nucleated from TB_{1st} ahead of crack tip. As we know, dislocation accommodation is an effective toughening mechanism for crack blunting, so GB_{1st} is intrinsically tough while TB_{1st} is intrinsically brittle due to different dislocation behaviours.

To illustrate the above observations, Figure 7(a) and (b) shows stress contours ($\sigma_{xy}, \sigma_{yy}, \sigma_{mean}$) near the crack-tip region in HTS ($\lambda_1 = 20.87$ nm, $\lambda_2 = 4.17$ nm) at two different strains, which are just right before nucleation of new voids from TB_{1st}. As shown from Figure 7(a), the shear stress σ_{xy} is highly inhomogeneous along the crack line, namely much higher at GB_{1st} for nucleation of partial dislocations while lower at TB_{1st} for possible nucleation of new voids. It is observed that both the mean stress σ_{mean} and the tensile stress σ_{yy} have peak values at one site of TB_{1st}, which is at a certain distance ahead of the crack tip. When the stress level around this site reaches a certain critical level, new void is created. When this void grows to a certain size, a second void is about to nucleate ahead of the existing void at another site of TB_{1st} for the same reason (Figure 7(b)).

Figure 8(a) and (b) shows a sequence of simulated snapshots illustrating crack propagation along the boundaries of primary twins in HTS ($\lambda_1 = 20.87$ nm, $\lambda_2 = 2.09$ nm). It is observed that crack resistance in HTS with small λ_2 is really high, and the crack growth includes only two stages: (i) initial crack growth along first TB_{1st} (Figure 8(a)); and (ii) crack-tip blunting at GB_{1st} (Figure 8(b)). In Figure 8(a), the early stage of crack-tip blunting is also observed after the initial crack growth along first TB_{1st}, so few dislocation slips are shown around the crack tip. In the second stages, the late stage of crack-tip blunting is accommodated by various dislocation behaviours around the crack tip as shown in Figure 8(c): (i) partial dislocations emitted from the crack tip travel across TB_{2nd}; (ii) partial dislocations emitted from the crack tip travel parallel to TB_{2nd}, leading to detwinning of secondary twins; (iii) partial dislocations emitted from GB_{1st} travel across SF; (iv) partial dislocations emitted from GB_{1st} travel parallel to TB_{2nd}, leading to detwinning of secondary twins; and (v) partial dislocations emitted

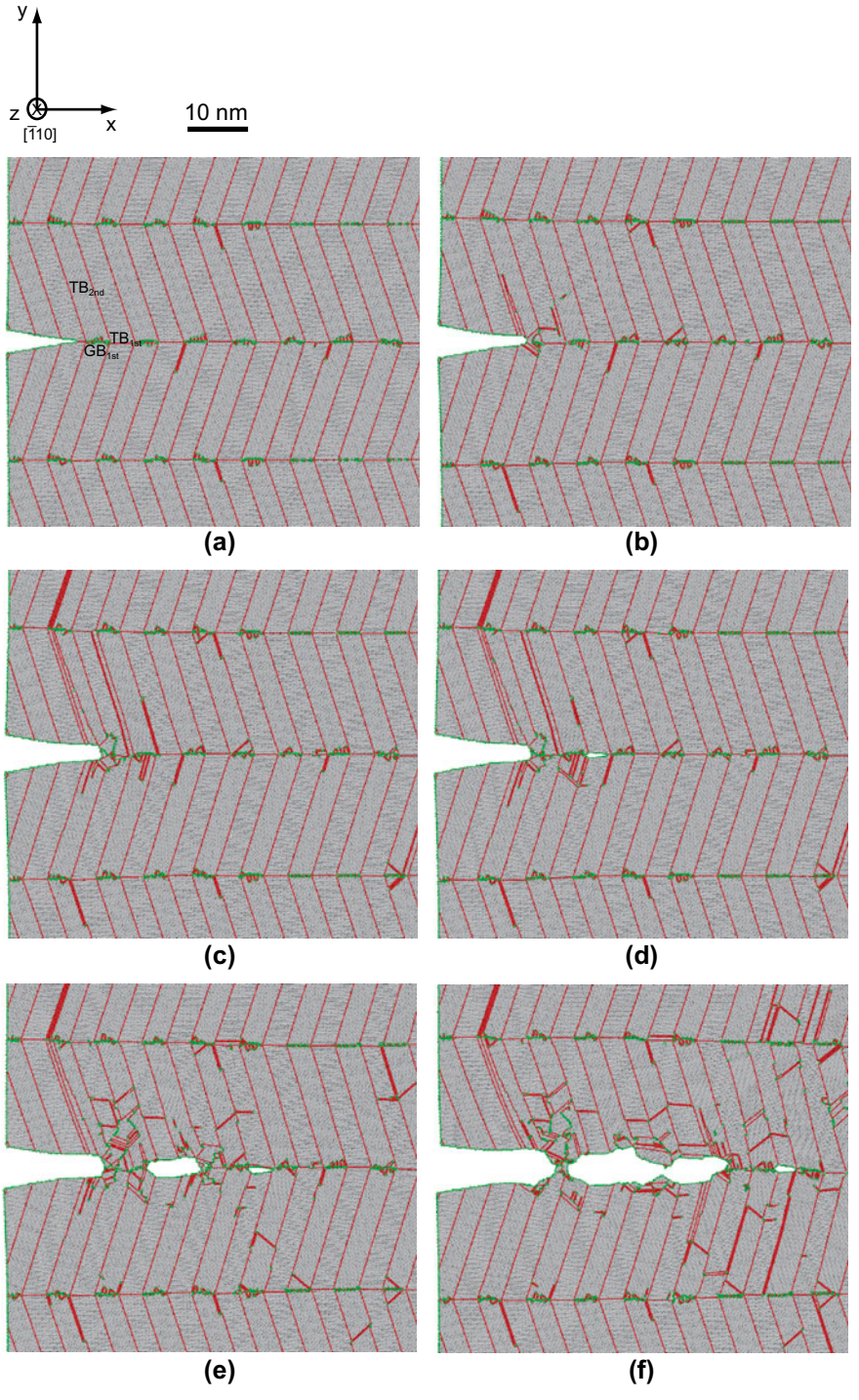

Figure 6. (colour online) Simulated snapshots illustrating crack propagation along the boundaries of primary twins in hierarchically twinned structures ($\lambda_1 = 20.87$ nm, $\lambda_2 = 4.17$ nm): (a) at a strain of 2.7%; (b) at a strain of 5.0%; (c) at a strain of 6.0%; (d) at a strain of 6.2%; (e) at a strain of 6.8%; (f) at a strain of 8.0%.

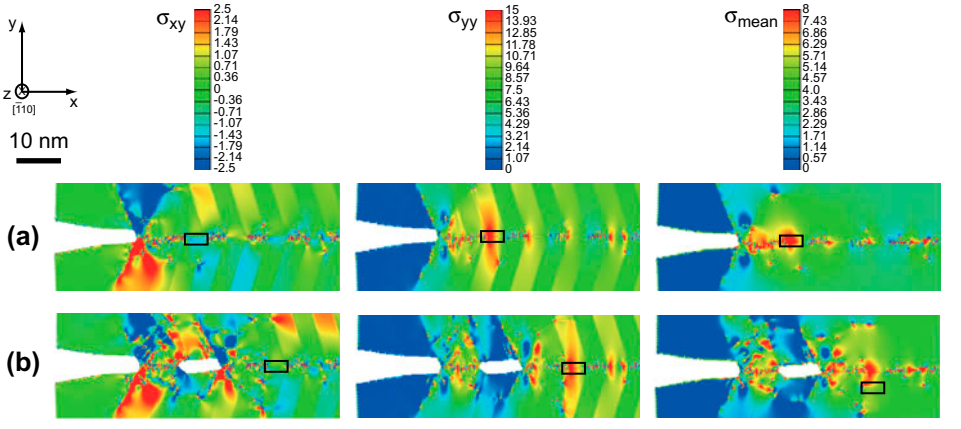

Figure 7. (colour online) Stress contours ($\sigma_{xy}, \sigma_{yy}, \sigma_{mean}$) near the crack-tip region of hierarchically twinned structures ($\lambda_1 = 20.87$ nm, $\lambda_2 = 4.17$ nm): (a) at a strain of 6.1%; (b) at a strain of 6.7%. The marked rectangular areas represent sites of TB_{1st} for nanovoids to nucleate at next step.

from TB_{2nd} travel across other TB_{2nd}. Unlike general GBs, TBs with low excess energies usually exhibit much higher thermal and mechanical stability. So, TBs can provide adequate barriers to dislocation motion for strengthening and also create more local sites for nucleating and accommodating dislocations, thereby improving ductility and work hardening [23]. However, dislocations nucleated from TBs are rarely observed in both experiments and MD simulations. Here, we show that TBs could provide local sites for both nucleating and accommodating dislocations. These dislocation behaviours provide an effective way to release the stress concentration around the crack tip and enhance the fracture toughness.

4. Summary

In the present study, a series of large-scale MD simulations have been performed to investigate the atomistic scale fracture behaviours along the boundaries of primary twins in Cu with HTS, and compare their fracture behaviours with those in monolithic twins. The results indicate that crack propagation along $[1\ \bar{1}\ \bar{2}]$ on the twin plane in monolithic nanotwins is brittle cleavage and fracture, resulting in low crack resistance and fracture toughness. However, the crack resistance along the boundaries of primary twins in HTS is much higher, and a smaller spacing of secondary twins (λ_2) leads to even higher fracture toughness. With large λ_2, the crack growth is achieved by four stages: (i) initial crack growth along first TB_{1st}; (ii) crack-tip blunting at GB_{1st}; (iii) void nucleation and growth from other sites of TB_{1st}; and (iv) void coalescence and crack growth. However, the crack growth includes only two stages when λ_2 is small: (i) initial crack growth along first TB_{1st}; and (ii) crack-tip blunting at GB_{1st}. Moreover, considerable plastic deformation and enhanced fracture toughness in HTS could be achieved by the crack blunting and by the extensive dislocation accommodation ahead of the crack tip when λ_2 is small.

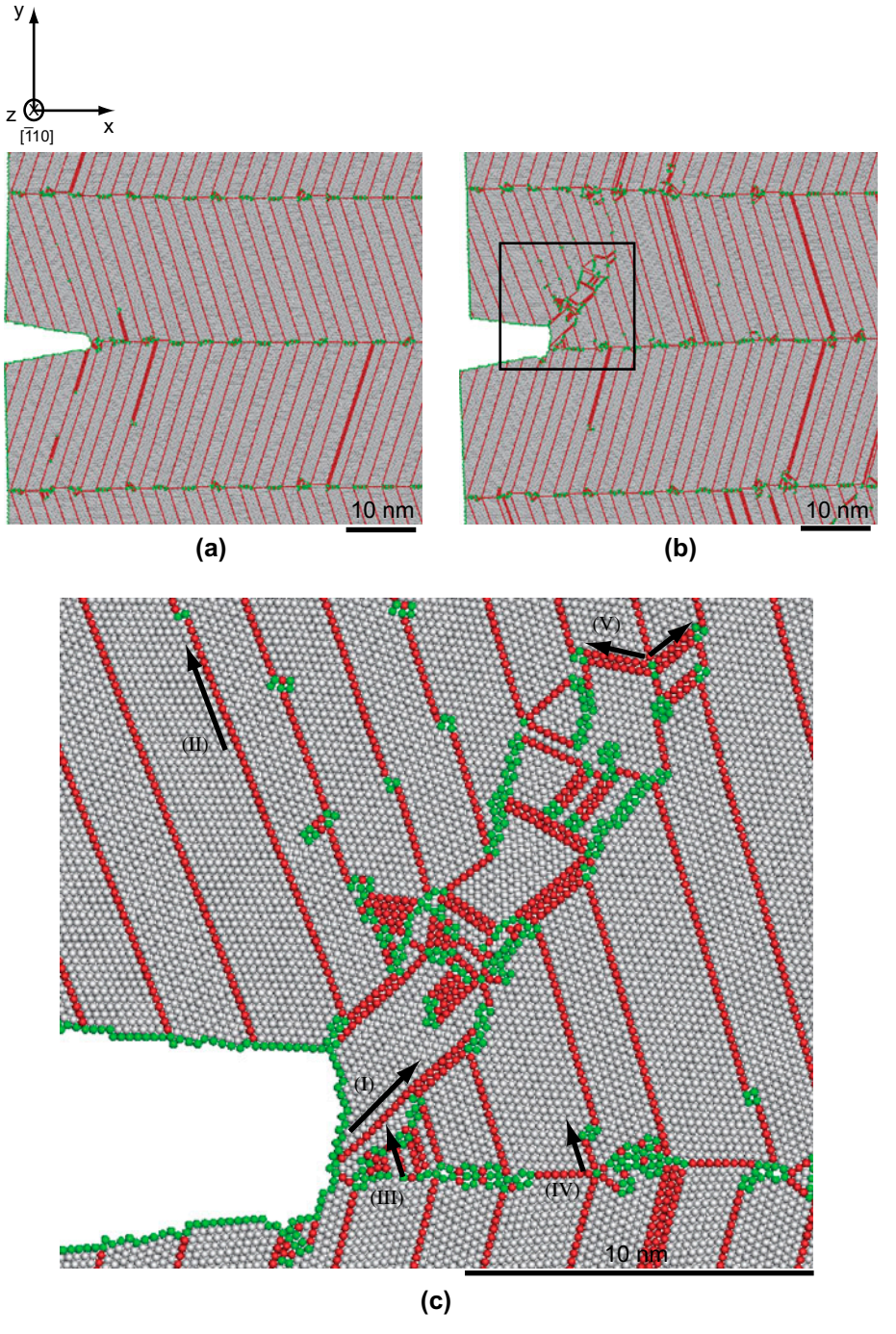

Figure 8. (colour online) Simulated snapshots illustrating crack propagation along the boundaries of primary twins in hierarchically twinned structures ($\lambda_1 = 20.87$ nm, $\lambda_2 = 2.09$ nm): (a) at a strain of 6.0%; (b) at a strain of 8.5%. (c) The corresponding amplified configuration for the marked rectangular area in Figure 7(b) to show the details for various dislocation behaviours around the crack tip.

Acknowledgements

The authors would like to acknowledge the financial support of the National Key Basic Research Program of China (Grants No. 2012CB932203 and No. 2012CB937500) and NSFC (Grants No. 11002151, No. 11222224, No. 11072243 and No. 11021262). The simulations reported were performed at Supercomputing Center of Chinese Academy of Sciences.

References

[1] A.A. Griffith, Philos. Trans. 221 (1921) p.163.
[2] G.R. Irwin, J. Appl. Mech. 24 (1957) p.361.
[3] M.L. Williams, J. Appl. Mech. 24 (1957) p.109.
[4] J.W. Hutchinson, J. Mech. Phys. Solids 16 (1968) p.13.
[5] J.R. Rice and G.F. Rosengren, J. Mech. Phys. Solids 16 (1968) p.1.
[6] S. Kohlhoff, P. Gumbsch and H.F. Fischmeister, Philos. Mag. A 64 (1991) p.851.
[7] F.F. Abraham, D. Schneider, B. Land, D. Lifka, J. Skovira, J. Gerner and M. Rosenkrantz, J. Mech. Phys. Solids 45 (1997) p.1461.
[8] S.J. Zhou, D.M. Beazley, P.S. Lomdahl and B.L. Holian, Phys. Rev. Lett. 78 (1997) p.479.
[9] D. Holland and M. Marder, Phys. Rev. Lett. 80 (1998) p.746.
[10] D. Holland and M. Marder, Adv. Mater. 11 (1999) p.793.
[11] D. Farkas, Philos. Mag. A 80 (2000) p.1425.
[12] D. Farkas, Mater. Res. Soc. 25 (2000) p.38.
[13] F.F. Abraham, J. Mech. Phys. Solids 53 (2005) p.1071.
[14] D. Farkas, Philos. Mag. 85 (2005) p.387.
[15] D. Farkas, S.V. Petegem, P.M. Derlet and H.V. Swygenhoven, Acta Mater. 53 (2005) p.3115.
[16] F. Rosch, H.R. Trebin and P. Gumbsch, Philos. Mag. 86 (2006) p.1015.
[17] S.W. Xu and X.M. Deng, Nanotechnology 19 (2008) p.115706.
[18] Y. Cheng, Z.-H. Jin, Y.W. Zhang and H. Gao, Acta Mater. 58 (2010) p.2293.
[19] H.F. Zhou, S.X. Qu and W. Yang, Modell. Simul. Mater. Sci. Eng. 18 (2010) p.065002.
[20] H.F. Zhou and S.X. Qu, Nanotechnology 21 (2010) p.035706.
[21] D.C. Jang, X.Y. Li, H.J. Gao and J.R. Greer, Nat. Nanotechnol. 7 (2012) p.594.
[22] F.P. Yuan and X.L. Wu, Phys. Rev. B 86 (2012) p.134108.
[23] Y.T. Zhu, X.Z. Liao and X.L. Wu, Prog. Mater Sci. 57 (2012) p.1.
[24] E.W. Qin, L. Lu, N.R. Tao and K. Lu, Scripta Mater. 60 (2009) p.539.
[25] E.W. Qin, L. Lu, N.R. Tao, J. Tan and K. Lu, Acta Mater. 57 (2009) p.6215.
[26] Y.T. Zhu, J. Narayan, J.P. Hirth, S. Mahajan, X.L. Wu and X.Z. Liao, Acta Mater. 57 (2009) p.3763.
[27] L. Lu, Y.F. Shen, X.H. Chen, L.H. Qian and K. Lu, Sicence 304 (2004) p.422.
[28] N.R. Tao and K. Lu, J. Mater. Sci. Technol. 23 (2007) p.771.
[29] Y.S. Li, N.R. Tao and K. Lu, Acta Mater. 56 (2008) p.230.
[30] K. Lu and J. Lu, Mater. Sci. Eng. A 375–377 (2004) p.38.
[31] K. Wang, N.R. Tao, G. Liu, J. Lu and K. Lu, Acta Mater. 54 (2006) p.5281.
[32] T.H. Fang, W.L. Li, N.R. Tao and K. Lu, Science 331 (2011) p.1587.
[33] H.N. Kou, PhD dissertation, The Hong Kong Polytechnic University, 2011.
[34] N.R. Tao and K. Lu, Scr. Mater. 60 (2009) p.1039.
[35] Y. Mishin, M.J. Mehl, D.A. Papaconstantopoulos, A.F. Voter and J.D. Kress, Phys. Rev. B 63 (2001) p.224106.
[36] H. Tsuzuki, P.S. Branicio and J.P. Rino, Comput. Phys. Commun. 177 (2007) p.518.